






A redistribution of nitrogen fertiliser across global croplands can help achieve food security within environmental boundaries

Andrew Smerald ¹✉, David Kraus¹, Jaber Rahimi ¹, Kathrin Fuchs ¹, Ralf Kiese ¹, Klaus Butterbach-Bahl ^{1,2} & Clemens Scheer¹

A major societal challenge is to produce sufficient food for a growing global population while simultaneously reducing agricultural nitrogen pollution to within safe environmental boundaries. Here we use spatially-resolved, process-based simulations of cereal cropping systems (at 0.5° resolution) to show how redistribution of nitrogen fertiliser usage could meet this challenge on a global scale. Focusing on major cereals (maize, wheat and rice), we find that current production could be (i) maintained with a 32% reduction in total global fertiliser use, or (ii) increased by 15% with current nitrogen fertiliser levels. This would come with substantial reductions in environmental nitrogen losses, allowing cereal production to stay within environmental boundaries for nitrogen pollution. The more equal distribution of nitrogen fertiliser across global croplands would reduce reliance on current breadbasket areas, allow regions such as Sub-Saharan Africa to move towards self-sufficiency and alleviate nitrogen pollution in East Asia and other highly fertilised regions.

¹Institute of Meteorology and Climate Research, Atmospheric Environmental Research (IMK-IFU), Karlsruhe Institute of Technology (KIT), Kreuzteckbahnstr. 19, 82467 Garmisch-Partenkirchen, Germany. ²Pioneer Center Land-CRAFT, Department of Agroecology, Aarhus University, Aarhus, Denmark.
✉email: andrew.smerald@kit.edu

The industrial fixation of atmospheric dinitrogen (N_2) for synthetic fertiliser production has been credited with feeding 40–50% of the current world population¹. However, this has resulted in a massive perturbation of the global nitrogen (N) cycle^{1–3}. The input of reactive nitrogen (denoted N_r and including all N species except N_2) to terrestrial ecosystems has increased from ~100 TgNyr⁻¹ in 1860 (mostly from natural sources) to a present value of 286 TgNyr⁻¹, of which 110 TgNyr⁻¹ originates from synthetic fertilisers^{2–4}. The resulting accumulation of N_r in the atmosphere, biosphere and hydrosphere is driving climate change, ozone depletion, biodiversity loss and eutrophication^{3,5}. In order to bring human activity back into its “safe operating space”^{6–8}, it has been estimated that anthropogenic N_r creation needs to be reduced to no more than 60–100 TgNyr⁻¹^{7,9}, although this could be increased to 130 TgNyr⁻¹¹⁹. Reconciling the need to reduce the effects of environmental N_r pollution with the need to feed the world population is here referred to as the “ N_r challenge”. A key part of meeting this challenge involves reducing the flows of the most harmful forms of N_r into the environment. These include nitrous oxide (N_2O), whose increasing atmospheric concentration accounts for about 6% of the radiative forcing responsible for global warming¹⁰ and ammonia (NH_3) and nitrate (NO_3^-), which are responsible for degrading ecosystems on a local to regional scale, as well as indirectly contributing to rising N_2O levels^{11–13}.

The three major food crops, maize, wheat and rice, account for >60 TgNyr⁻¹ of synthetic N fertiliser use, ~60% of the global total¹⁴. At the same time, they directly contribute ~50% of globally consumed calories, as well as ~12% of all livestock feed¹⁴. Reducing the N_r input to cereal agroecosystems while maintaining or increasing yields is thus a crucial part of mitigating the N_r challenge, which is expected to further intensify due to a rapidly growing global demand for crops^{15–17}, potentially by 35–56% between 2010 and 2050¹⁸. However, it is worth noting that actual crop demand could be considerably lower in the case of largescale adoption of more plant-based diets and/or reduction of food spoilage and waste^{19–21}.

Here, we use the process-based biogeochemical model LandscapeDNDC (LDNDC)²² to show that considerable mitigation of the N_r challenge is possible by redistributing N fertiliser usage on a global scale, i.e. prioritising N fertiliser application in locations where it has the largest effect on cereal yields, resulting in yield increases in some regions and yield decreases in others. We adopt a target date of 2030, and additionally build into the N fertiliser redistribution strategy the conditions that: (1) the NO_3^- concentration in soil water leachate does not exceed the critical load of 2.5 mgNl⁻¹, beyond which aquatic ecosystem degradation is likely^{7,9,23}, and (2) there is no change in the distribution of arable

land (both conditions are enforced at the 0.5° grid cell level). Within this framework, we evaluate two main scenarios (see Table 1) relative to the *baseline* (which models agricultural conditions in 2015): (1) the *low emission* scenario prioritises reductions in N_2O emissions consistent with the goal of limiting global warming to 1.5°C²⁴; (2) the *high yield* scenario prioritises increases in cereal production consistent with the upper end of predicted crop demand in 2030¹⁸. In addition, we evaluate a *maintain regional production* scenario, which builds on the *high yield* scenario but avoids decreases in cereal production relative to the *baseline* scenario in (sub-) continental regions.

Since we are considering only a short timescale (i.e. 2015–2030), we have assumed that agricultural conditions typical of 2015 are relevant for the entire period. This includes the assumption that changes in the climate and atmospheric CO_2 concentrations won't lead to a large change in cereal yields, which is consistent with previous work on the effect of climate change and increased CO_2 fertilisation on cereal yields before 2030²⁵. It also includes the assumption that irrigation and field management strategies (except for fertiliser usage) remain constant. Another important assumption is that phosphorous, potassium and other plant nutrients are supplied commensurately with N, and are therefore not limiting factors for crop growth.

Results and discussion

Quantifying the N_r challenge. In our simulations of current agricultural practice (*baseline* scenario in Table 1 and Figs. 1–3), 62 TgNyr⁻¹ (22 TgNyr⁻¹ to maize, 21 TgNyr⁻¹ to wheat and 19 TgNyr⁻¹ to rice) is supplied as synthetic fertiliser²⁶ and 8 TgNyr⁻¹ as manure²⁷, resulting in a total global production of maize, wheat and rice of 2570 Tgyr⁻¹ (950 Tgyr⁻¹ of maize, 720 Tgyr⁻¹ of wheat and 900 Tgyr⁻¹ of rice). This is in good agreement with the FAO estimate of 2520 Tgyr⁻¹ (1050 Tgyr⁻¹ of maize, 730 Tgyr⁻¹ of wheat and 740 Tgyr⁻¹ of rice)¹⁴. Associated N_2O emissions are 1.0 TgNyr⁻¹ (0.42 TgNyr⁻¹ from maize, 0.35 TgNyr⁻¹ from wheat and 0.26 TgNyr⁻¹ from rice), consisting of 0.76 TgNyr⁻¹ of direct emissions from agricultural soils and 0.25 TgNyr⁻¹ of indirect emissions due to the conversion of NO_3^- and NH_3 to N_2O in the wider environment. N_2O emissions thus correspond to ~15% of the estimated 7 TgNyr⁻¹ of total anthropogenically generated emissions²⁸. Global NO_3^- leaching losses amount to 14.5 TgNyr⁻¹ (6.0 TgNyr⁻¹ from maize, 5.6 TgNyr⁻¹ from wheat and 2.9 TgNyr⁻¹ from rice), corresponding to 21% of the applied N. As a result, water leachate from 40% of the total harvested area, accounting for 48% of total production, has an NO_3^- concentration exceeding the critical

Table 1 Results of scenario runs for improving the efficiency of N fertiliser usage in cereal agroecosystems.

Scenario name	Scenario assumptions and constraints	Crop production (Tgyr ⁻¹)	Synthetic fertiliser usage (TgNyr ⁻¹)	NO_3^- leaching (TgNyr ⁻¹)	N_2O emissions (TgNyr ⁻¹)
<i>Baseline</i>	• Circa 2015 conditions	2580	62	14.5	1.02
<i>Low emission</i>	• N_2O : 29% reduction in emissions • NO_3^- : soil water leachate contains <2.5 mgNl ⁻¹ in every grid cell	2640 (+2%)	42 (-32%)	6.2 (-57%)	0.72 (-29%)
<i>High yield</i>	• Production: 15% increase • NO_3^- : soil water leachate contains <2.5 mgNl ⁻¹ in every grid cell	2960 (+15%)	63 (+2%)	7.8 (-46%)	0.97 (-5%)
<i>Maintain regional production</i>	• Production: <i>High yield</i> plus every region maintains at least 2015 levels of crop production	3050 (+18%)	70 (+13%)	10.5 (-28%)	1.06 (+4%)

The *baseline* scenario models cereal agriculture (maize, wheat and rice) in current conditions. All other scenarios redistribute N-fertiliser application rates on a global scale so as to maximise cereal production, given the scenario assumptions and constraints. Percentages in brackets show the difference from the *baseline*. Supplementary Table 9 shows the same information broken down by crop type.

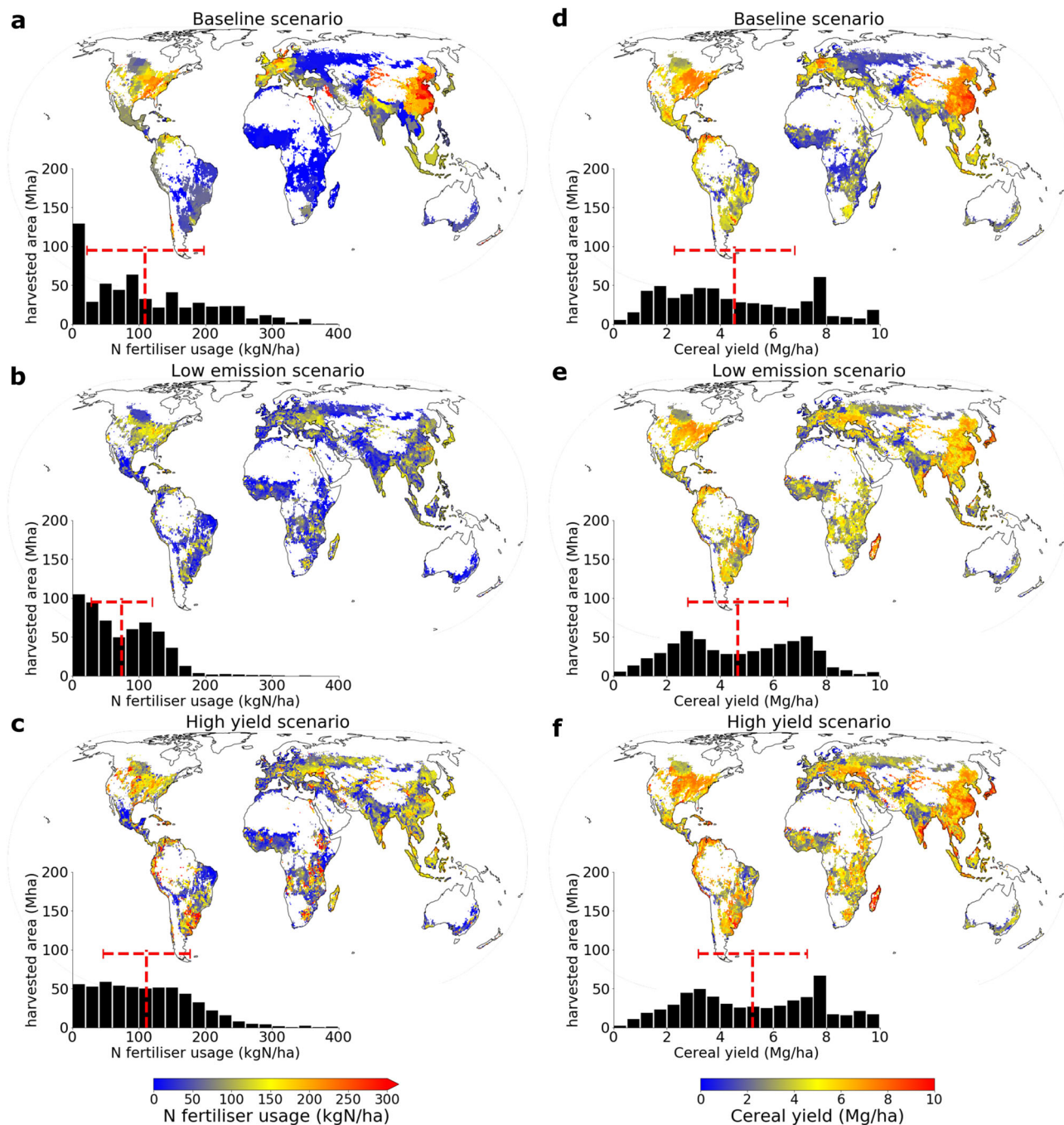


Fig. 1 Synthetic N fertiliser usage and cereal yields before and after fertiliser redistribution. Maps of N-fertiliser application rates (**a**, **b** and **c**) and cereal yields (**d**, **e** and **f**), for the *baseline* (**a**, **d**), *low emission* (**b**, **e**) and *high yield* (**c**, **f**) scenarios (see Table 1 for scenario descriptions). Black bars show the distribution of harvested areas vs. N application rates or cereal yields. Red dashed lines represent the global mean and standard deviation. Difference maps are shown in Supplementary Fig. 7 and maps of global harvested areas in Supplementary Fig. 8.

load ($>2.5 \text{ mgNi}^{-1}$) at which ecosystem degradation becomes likely (see Fig. 2). Water leachate from 7% of the harvested area, accounting for 9% of production, is considered unsafe for human consumption ($>11 \text{ mgNi}^{-1}$)²⁹. For more details on the evaluation of results see Supplementary Note 1.

A large fraction of current cereal production is concentrated in North America, East Asia and Europe (see Fig. 1). These regions account for 53% of production, despite only containing 38% of the global harvested area. On the other hand, Sub-Saharan Africa accounts for 9% of the global harvested area but only 4% of production. One reason for this production disparity is the

inequality in N fertiliser application rates. Synthetic N fertiliser usage in North America ($143 \text{ kgNha}^{-1}\text{cropping-season}^{-1}$), East Asia ($236 \text{ kgNha}^{-1}\text{cropping-season}^{-1}$) and Europe ($94 \text{ kgNha}^{-1}\text{cropping-season}^{-1}$) accounts for 62% of total global usage, as compared to $<1\%$ in Sub-Saharan Africa ($11 \text{ kgNha}^{-1}\text{cropping-season}^{-1}$). Unsurprisingly, high environmental N losses are likewise concentrated in North America, East Asia and Europe, which account for 56% of N_2O emissions and 54% of NO_3^- leaching. In these regions the NO_3^- concentration of water leachate exceeds 2.5 mgNi^{-1} across 58% of the harvested area. On the other hand, agricultural land in Sub-Saharan Africa only

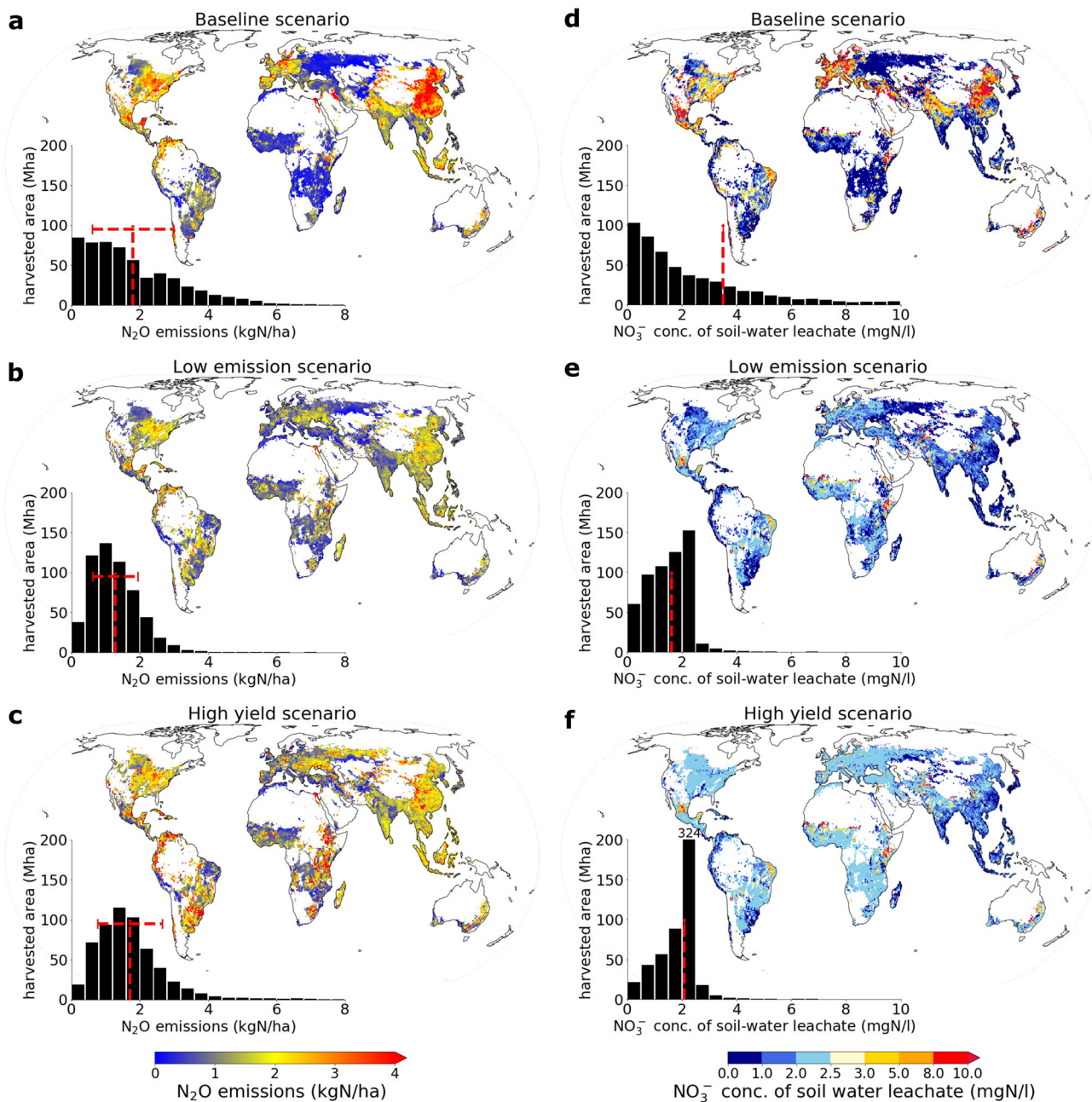


Fig. 2 N_2O emissions and NO_3^- leaching before and after N fertiliser redistribution. Maps of N_2O emission rates (a, b and c) and NO_3^- concentration of soil water leachate (d, e and f), for the baseline (a, d), low emission (b, e) and high yield (c, f) scenarios (see Table 1 for scenario descriptions). Black bars show the distribution of harvested areas vs. N_2O emission rates or NO_3^- concentrations. Red dashed lines represent the global mean and standard deviation (no standard deviation is shown for NO_3^- concentrations due to the long tailed nature of the distribution).

contributes marginally to global environmental N losses from cereal cropping systems, with 3% of global N_2O emissions and 2% of NO_3^- leaching (only 11% of the harvested area has N leaching exceeding 2.5 mgNl^{-1}).

Opportunities for meeting the N_r challenge. The global disparity in N-fertiliser usage (see Fig. 1), coupled with the highly non-linear relationships between fertiliser usage, cereal yields and environmental N losses in the form of N_2O emissions and NO_3^- leaching, suggests that global fertiliser redistribution has a high potential to mitigate the global N_r challenge. In the *low emission* scenario, redistribution allows cereal production to be maintained at current levels, despite a reduction in global N fertiliser usage from 62 to 42 TgNyr^{-1} (15 TgNyr^{-1} for maize, 11 TgNyr^{-1} for

wheat and 16 TgNyr^{-1} for rice). Considering a safe budget of 60–100 TgNyr^{-1} ¹⁷, this leaves a remaining budget of 20–60 TgNyr^{-1} for all other anthropogenic N fixation, including fertilisation of other crops, biological N fixation by leguminous crops and NO_x creation during combustion processes⁴. In this scenario, N_2O emissions are reduced by 29% compared to the *baseline* (29% for maize, 40% for wheat and 13% for rice), in line with what is required by 2030 to limit global warming to 1.5°C ²⁴. The NO_3^- concentration of soil-water leachate is reduced below 2.5 mgNl^{-1} over 96% of the harvested area (see Fig. 2), and this corresponds to a 57% reduction in NO_3^- leaching (62% for maize, 71% for wheat and 24% for rice).

On a (sub-) continental scale (see Fig. 3) the *low emission* scenario implies large reductions in N fertiliser usage in East Asia

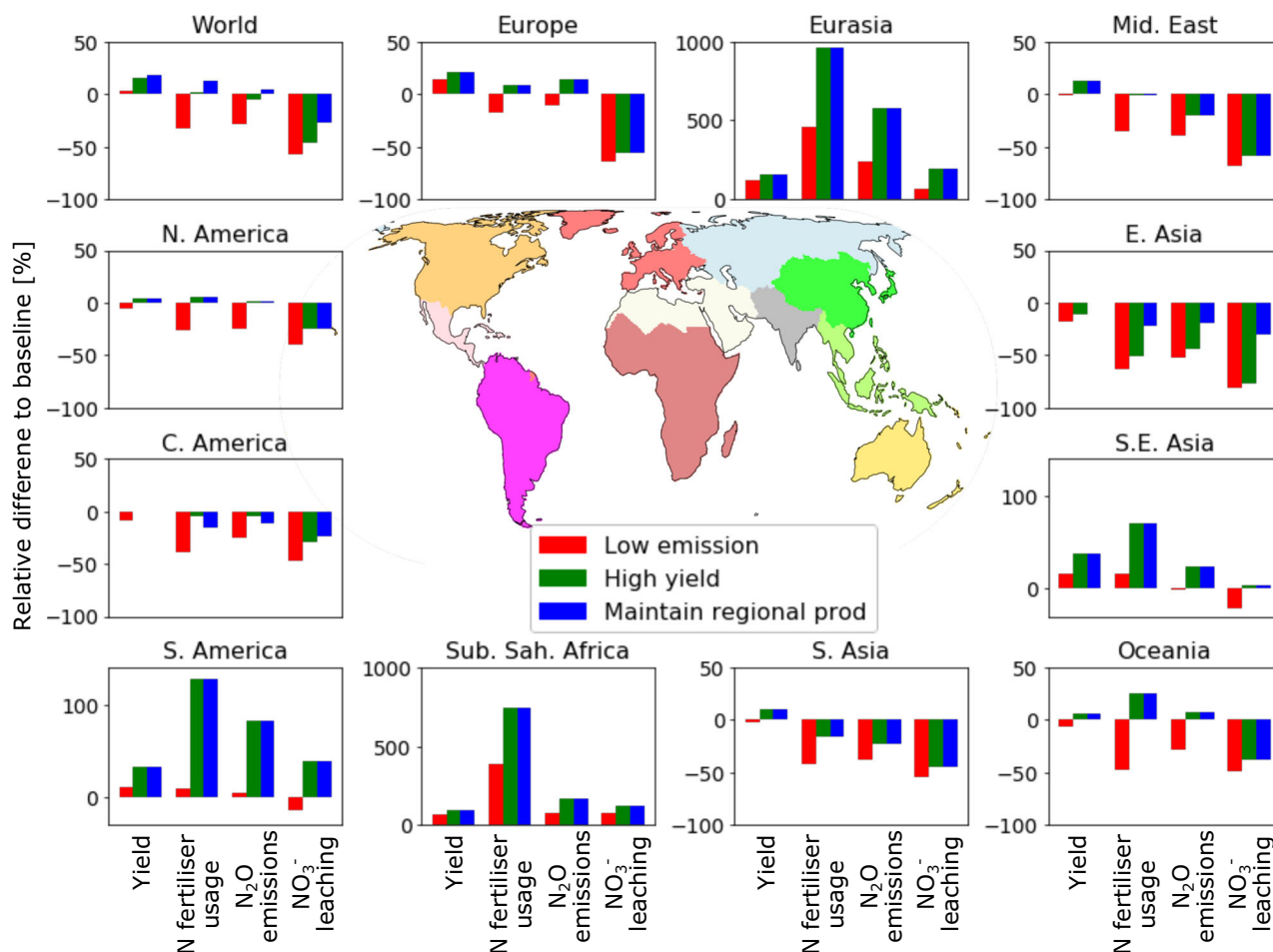


Fig. 3 Regional changes in cereal yield, N-fertiliser usage, N₂O emissions and NO₃⁻ leaching. Changes are shown relative to the *baseline* scenario (see also Supplementary Fig. 12 and Supplementary Tables 1-5).

(236 to 88 kgNha⁻¹cropping-season⁻¹) and North America (143 to 107 kgNha⁻¹cropping-season⁻¹). This results in relatively modest reductions in production (−18% in East Asia and −6% in North America), but a substantial reduction in environmental N pollution (NO₃⁻ leaching: East Asia: −81% or 7.1 to 1.2 mgNl⁻¹; North America: −40% or 2.8 to 1.7 mgNl⁻¹; N₂O emissions: East Asia: −53%; North America: −25%). Yield decreases in intensively farmed regions are outweighed by increases in regions such as Sub-Saharan Africa and Eurasia, where modest increases in average N fertiliser application rates (Sub-Saharan Africa 11 to 54 and Eurasia 11 to 59 kgNha⁻¹cropping-season⁻¹) result in large yield increases (+67% and +123%).

Of the three crops, wheat shows the highest potential to reduce N fertiliser usage and Nr losses without reducing global yields, with a 45% reduction in N fertiliser usage, 40% reduction in N₂O emissions and 71% reduction in NO₃⁻ leaching. This is achieved by balancing reductions in wheat yields in South Asia, East Asia and Western Europe with increases in Eastern Europe and Northern Asia (see Supplementary Figs. 9 and 10 and Supplementary Table 3). Maize also shows considerable potential, with a 33% reduction in N fertiliser usage, 29% reduction in N₂O emissions and 62% reduction in NO₃⁻ leaching. This is primarily driven by modest reductions in maize yields in East Asia and North America being compensated by increases in Sub-Saharan Africa (Supplementary Table 4). Rice shows much lower potential for changes in N fertiliser management to reduce Nr losses (Supplementary Table 5), but some reductions are possible by shifting production from East to South-East Asia. However, losses

of N₂O and NO₃⁻ are currently much lower than in wheat and maize fields. This is due to common management practices that result in soil compaction and water saturation, reducing the percolation rate and promoting complete denitrification of NO₃⁻ to N₂ rather than N₂O.

In the *high yield* scenario, N fertiliser redistribution allows cereal production to be increased by 15% by 2030 (i.e. in line with the upper end of predicted demand) without increasing global N fertiliser usage, which remains at just over 60 TgNyr⁻¹ (21 TgNyr⁻¹ for maize, 20 TgNyr⁻¹ for wheat and 22 TgNyr⁻¹ for rice). As a result, large cuts in other anthropogenic N_r fixation pathways, such as fossil fuel combustion (currently 30 TgNyr⁻¹)⁴ or agricultural biological N fixation (currently 60 TgNyr⁻¹)⁴, would be necessary to stay within the safe budget of 60–100 TgNyr⁻¹. N₂O emissions in the *high yield* scenario show a small reduction of −5% (−8% for maize, −6% for wheat and +4% for rice), consistent with some, but not all, of the IPCC scenarios for limiting global warming to 1.5 °C²⁴. NO₃⁻ leaching nearly halves (−50% for maize, −59% for wheat and −14% for rice), and, as in the *low emission* scenario, is below the critical threshold of 2.5 mgNl⁻¹ on over 96% of the harvested area.

In the *high yield* scenario, East Asia is the only region where cereal production is reduced (−11%, see Fig. 3), due to a 51% decrease in N fertiliser usage (to 117 kgNha⁻¹cropping-season⁻¹). However, this results in a 44% reduction in N₂O emissions and a 77% decrease in NO₃⁻ leaching. Large production increases occur in Sub-Saharan Africa (+93%), the region with the highest predicted increase in food demand¹⁶, and

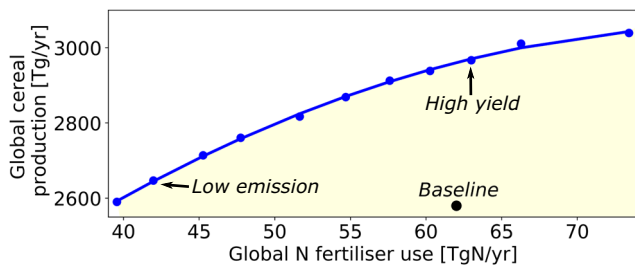


Fig. 4 The trade-off frontier between cereal production and N fertiliser usage. Blue dots show the global cereal production obtainable via optimal redistribution of N fertiliser on a global scale (i.e. the redistribution that maximises cereal production for a given quantity of N fertiliser). The yellow shaded region shows the wider, non-optimal space of possibilities for redistributing N fertiliser.

Eurasia (+159%), driven by increasing N fertilisation rates (to 94 and 114 kgNha⁻¹ cropping-season⁻¹ respectively).

Of the three crops, maize shows less potential for yield increases than wheat or rice, due to a combination of yield saturation and risks for NO₃⁻ leaching. Large global reductions in NO₃⁻ leaching from maize fields are mostly due to reductions in N fertiliser usage in East Asia, while compensatory increases in, for example, Sub-Saharan Africa lead to only modest increases in NO₃⁻ leaching (see Supplementary Figs. 9 and 11 and Supplementary Table 3). For wheat, the relatively modest increases in yield between the *low emission* and the *high yield* scenario (+14%) require a large increase in N fertiliser usage (+80%). Nevertheless, NO₃⁻ leaching can be kept within environmental limits by directing a higher fraction of N fertiliser to Eurasia as opposed to South and East Asia, where current N fertilisation levels are very high (see Supplementary Table 4). For rice, where N₂O emissions and NO₃⁻ leaching are already low compared to wheat and maize, modest decreases in NO₃⁻ leaching are possible by reducing N fertiliser levels in East Asia, while increasing them in South and in particular South-East Asia (see Supplementary Table 5).

In order to illustrate further options associated with N fertiliser redistribution, we map out a trade-off frontier in Fig. 4. This gives a snapshot of the maximum possible agronomic efficiency given current agricultural technologies, and would be expected to evolve over time^{30,31}. At the frontier, N fertiliser is globally redistributed so as to maximise crop production, and the *low emission* and *high yield* scenarios thus correspond to points on the frontier curve. Mapping out a frontier curve makes it clear that the efficiency with which N fertiliser is converted to cereal yields decreases with increasing cereal production, resulting in N losses increasing faster than yields (see Supplementary Fig. 13). In consequence, even small reductions in the demand for cereals, for example via dietary change or reduced food wastage, would have a large effect on N fertiliser usage and N losses.

The cost of maintaining crop production in East Asia. Reducing average cereal yields in East Asia, as occurs in both the *low emission* and *high yield* scenarios, would upset the region's current balance between production and consumption¹⁴, necessitating an increase in imports (assuming no reduction in consumption). In consequence, we have assessed the extent to which N fertiliser redistribution within East Asia would allow N pollution to be reduced while maintaining cereal yields (maintain regional production scenario). We find that current production could be achieved with 22% less N fertiliser usage. However, even though NO₃⁻ leaching in the region would be 31% lower than in the baseline case, NO₃⁻ pollution would remain a major concern, with >50% of the harvested area exceeding the critical load (2.5 mgNI⁻¹). This would predominantly

be driven by maize production (average of 57 kgNha⁻¹ of leaching across a total harvested area of 45.4 Mha), as opposed to rice production (average of 14 kgNha⁻¹ of leaching across 33.7 Mha of harvested area). Our results thus suggest that, without additional changes to agricultural management practices, East Asia cannot produce sufficient cereals to meet current demand while avoiding the consequences of NO₃⁻ pollution.

Implications and caveats. Efficient N fertiliser redistribution would alter the global distribution of cereal production (see Fig. 1), changing trade patterns and food self-sufficiency levels. One important effect would be a reduction in the global reliance on breadbasket regions such as the US Midwest or Eastern China (Figure 1 shows that, relative to the *baseline*, the *low emission* and *high yield* scenarios have smaller standard deviations in their yield distributions, implying a more even distribution of yields across farmland). This would reduce the impact of breadbasket failures³², which will likely become more frequent as the climate warms and extreme weather events such as drought become more common³³. On average, it would also reduce disruption to the global food system caused by regional conflicts. However, this is not guaranteed, as highlighted by the current war in Ukraine, which is among the regions with the highest potential to increase cereal yields, especially of wheat.

At the regional level, the most obvious beneficiary of N fertiliser redistribution would be Sub-Saharan Africa, which currently produces only 72% of the cereals it consumes¹⁴ and is particularly vulnerable to volatility in global food markets³⁴. Even in the more conservative *low emission* scenario, the increase in cereal production would allow it to become self-sufficient at current consumption levels, and also partially satisfy the predicted rapid rise in demand¹⁶. On the other hand, Central America and North Africa/Middle East show only limited potential to increase production by more efficient N fertiliser use, and so would remain heavily reliant on imports (current production levels are 58% and 54% of consumption¹⁴).

Increasing yields in regions such as Sub-Saharan Africa - often discussed in terms of yield-gap closing - has received considerable attention in the literature³⁵⁻³⁷. However, those studies that have considered the effect of yield gap closing on N flows³⁸⁻⁴² have neither put the flows into the context of safe boundaries for N losses, nor paired yield-gap closing with yield reductions in heavily fertilised regions. On the other hand, studies that have explored the consequences of enforcing N boundaries on a global scale have typically relied on exogenous assumptions for future developments in nitrogen use efficiency^{43,44}. In contrast, the key feature of our work is to provide a quantified scheme for how to improve the global efficiency with which N fertiliser is converted to cereal production (see Supplementary Note 2 for a more detailed comparison to past work).

Efficient conversion of N fertiliser into cereals is clearly a crucial part of the N_r challenge, since maize, wheat and rice agroecosystems receive 60% of synthetic N fertiliser¹⁴. As such, it is desirable to additionally pursue other strategies for increasing the conversion efficiency, many of which would interact constructively with spatial redistribution. For example, optimisation of the timing, placement and type of N fertiliser usage^{45,46}, improved residue management^{47,48} and large scale adoption of urease and nitrification inhibitors^{49,50}. At the same time, N_r stored in cereal grains remains in a reactive state, and careful management of both human waste and animal manure, especially from intensive livestock production⁵¹, is another key ingredient for mitigating the N_r challenge, since our study takes into account only the manure that is applied to cereal agroecosystems.

While we have concentrated on the trade-off between yields and N_r pollution, there are additional challenges associated both with closing yield gaps in sparsely fertilised regions and reducing yields in highly fertilised regions. For closing yield gaps, additional N fertiliser application may need to be paired with other changes in field management and/or the wider agricultural environment³⁶. For example, in addition to ensuring that nutrients such as phosphorous and potassium are supplied commensurately with N, it may also be necessary to improve the infrastructure for harvesting, transporting and storing crops⁵². On the other hand, reducing yields in currently high-yielding areas may be politically difficult. For example, farmers in the Netherlands have recently been resisting proposals by the government to reduce N pollution by cutting livestock numbers⁵³.

Our predictions for how N fertiliser could be optimally redistributed so as to reduce usage and therefore environmental N pollution could be improved by further refinements to the LDNDC model structure and by new data sources. For example, global datasets concerning common crop rotations and multi-cropping practices would improve our ability to model the effect of previous management on N and carbon budgets. Further work on the processes and parameters that govern maize and rice yields would also allow for improved predictions. Currently, predicted maize yields are 10% below FAO estimates and rice yields 20% above FAO estimates (see Supplementary Note 1). This suggests that N surplus (i.e. remaining N after plant N uptake) is on average overestimated for maize and underestimated for rice, resulting in over- (maize) and under- (rice) estimation of N_2O emissions and NO_3^- leaching. Improving model yields would therefore increase the potential for maize cultivation and decrease the potential for rice cultivation in the *low emission* and *high yield* scenarios. Furthermore, considering diseases, pests and weeds could improve modelled yields.

In conclusion, we have demonstrated that spatial redistribution of N fertiliser in cereal agroecosystems could alone allow for considerable mitigation of the N_r challenge by 2030. Since these systems account for ~1/3 of total anthropogenic N_r fixation³, this would provide a big step towards bringing N_r usage back within its safe operating space, and result in a more even spread of cereal production across global cropland. Finally, it is worth pointing out that spatial redistribution of N fertiliser at the global scale is not an all or nothing strategy. Even a partial implementation could bring substantial benefits in many regions, increasing food security while mitigating the effects of N_r on climate change and environmental pollution.

Methods

Model description. LandscapeDNDC is a model framework for the simulation of nitrogen, carbon and water flows within and between soil and plants and in exchange with the atmosphere and hydrosphere²². It is 1-D, process based and allows for the coupling of different sub-models. Here we use MeTr^x for simulating soil carbon and N turnover⁵⁴ and PlaMo^x for plant growth^{54–56}.

Crop yields. In the PlaMo^x submodel, plants are divided into four compartments—roots, stems, leaves and grains - and crop yields are determined by the grain biomass at harvest time. Carbon, which in the model is related to total biomass by a constant factor, enters the plant via a photosynthesis routine based on the modelling approaches of Farquhar et al.⁵⁷ and Ball et al.⁵⁸. The maximum rate of carbon intake is determined by a combination of leaf area, canopy structure, incoming radiation and atmospheric CO_2 levels, and this is further modified by N and water availability and temperature. Carbon accumulation depends on the difference between incoming

carbon from photosynthesis and carbon losses via respiration, root exudation and plant senescence. Accumulated carbon is dynamically allocated between roots, stems, leaves and grains, depending on the plant development stage, which is determined by the accumulation of growing degree days. Different crops share most of the same processes, but are parametrised differently and have small differences in the dynamical allocation of carbon to plant compartments. Additionally, the development of winter wheat is dependent on having sufficiently low winter temperatures to meet the need for vernalisation.

N_r losses. N_2O is produced during nitrification and denitrification processes. Nitrification occurs in the aerobic soil fraction, and the rate of N_2O production depends on the size, activity level and potential growth rate of the nitrifier population, pH, temperature, level of water saturation and NH_4^+ availability. Denitrification occurs in the anaerobic soil volume fraction, and the rate of combined N_2O and N_2 production depends on the size, activity level and potential growth rate of the denitrifier population and carbon and N availability. Larger anaerobic soil volume fractions lead to a higher total denitrification rate, but result in a smaller ratio of $N_2O:N_2$ production. N_2O produced via nitrification and denitrification diffuses through the soil column, and may be denitrified to N_2 before being emitted to the atmosphere.

NO_3^- leachate is carried by water percolating through the soil column. Water percolation is simulated via a cascading bucket model, and the rate depends on the soil hydraulic conductivity, wilting point and field capacity, as well as the relative water content of neighbouring soil layers⁵⁹. The leaching of NO_3^- is proportional to availability and to the ratio of percolated to total water in a soil layer. NO_3^- availability is itself dependent on the balance between input (fertilisation, deposition), production (nitrification) and consumption (plant uptake, microbial assimilation, denitrification) processes. NO_3^- leaching out of the bottom soil layer leaves the simulation and is considered to have leached into the ground water.

NH_3 is produced in an equilibrium reaction with NH_4^+ , with high pH values and temperatures favouring NH_3 . The availability of NH_4^+ is dependent on the balance between input (fertilisation, deposition), production (mineralisation) and consumption (plant uptake, microbial assimilation, nitrification) processes. As with N_2O , the movement of NH_3 through the soil column and into the atmosphere is modelled as a diffusion process.

Model calibration and validation

Field scale calibration and validation. LDNDC has been calibrated and validated against field-scale measurements across a variety of land-uses (arable^{54,55,60–64}, grassland^{56,61,65} and forest^{59,66,67}) and climates (temperate^{55,61}, tropical^{54,62,64} and savannah⁶⁸). Simultaneous calibration was performed across multiple sites and measurements, with a particular focus on N losses, especially of N_2O and NO_3^- ^{55,61,69,70}. Soil processes were parametrised consistently across different land-uses and climates^{55,61,70} and plant processes across different climates and soil types^{55,61}. The soil process description and parametrisation has been further improved using measurements of the stable isotope ^{15}N ^{65,71} (see Supplementary Tables 7 and 8 for values of key parameters).

Crucially for this study, calibration and validation of the model has been performed for highly varying N fertiliser application rates. In upland systems fertiliser application rates varied from ~20–300 $kgNha^{-1}yr^{-1}$ ¹⁶¹, and in paddy rice systems from 0–360 $kgNha^{-1}yr^{-1}$ ¹⁶², and the model was able to robustly simulate both crop yields and N losses across the full range of N inputs. Additionally, the soil process description and parametrisation has proven capable of simulating N losses across ecosystems with

highly varying N input rates, ranging from extensively managed forests^{66,67} (N deposition of 10–20 kgNha⁻¹yr⁻¹) to intensively managed grasslands⁵⁶ (up to 240 kgNha⁻¹yr⁻¹ of manure).

Regional validation. LDNDC has been used extensively for regional simulations, and has proven able to provide robust estimates for plant growth and N losses across varying scales and ecosystem types. This includes at the catchment^{60,63,70}, subnational^{22,72}, national^{64,73} and supranational scale⁴⁸. These regional studies included large differences in N fertiliser application rates. For example, European croplands were modelled with rates varying from 20–365 kgNha⁻¹⁴⁸.

Global calibration and validation. The only additional model calibration performed for global modelling was a grid-cell-specific crop cultivar selection⁴². This was done by matching the accumulated growing degree days required for crops to reach maturity to the average number of growing degree days between the planting and harvesting days in the crop calendar. The accumulated growing degree days required for other plant development stages (e.g. emergence, flowering, grain filling) were adjusted proportionally.

Previous use of LDNDC for global crop modelling has shown that it is comparable to other crop models for modelling crop yields, and in particular their climatic response²⁵. For this study we have performed a number of additional validation steps on the global scale. We compared (see Supplementary Note 1): (1) simulated crop yields to FAO data¹⁴ for country-specific yields in the year 2015; (2) simulated crop N contents to country-specific FAO data for 2015¹⁴, via measurements of the N use efficiency; (3) simulated direct soil N₂O emissions to a tier 1 emission factor approach applied on a country scale⁷⁴; (4) simulated NO₃⁻ leaching to a tier 1 leaching factor approach applied on a country scale⁷⁴; (5) simulated yield gaps due to nutrient deficiency to those estimated by the Global Agro-Ecological Zones project⁷⁵. In all cases a good agreement was found between the different approaches, suggesting that LDNDC is capable of accurately simulating both current yields and N losses and their response to changes in N fertiliser usage.

Model setup: The input data and setup were mostly chosen so as to be consistent with the Gridded Global Crop Model Inter-comparison (GGCMI) project, since this provides a collection of the most up-to-date data for global crop modelling²⁵. We focused on agricultural conditions in the year 2015, the most recent year for which all necessary input data is available. As is common in global crop modelling, only one growing season was simulated per calendar year, and crop rotations were not considered (thus we ignore the effect of N fixation by leguminous crops grown in rotation with cereals)^{25,31,43,76}. While multi-cropping was not explicitly simulated, it was taken into account in post-processing via the harvested area. As such, we ignore the interaction between subsequent crops. The N fertiliser application rates used for the *baseline* scenario combine subnational, crop-specific data for large producer countries (e.g. China, USA, India, Western Europe) with national rates for countries where no better data is available (e.g. large parts of Africa)²⁶. The data is based upon the N fertiliser application rates reported in Mueller et al.³⁹, updated using the Land Use Harmonisation 2 dataset⁷⁷. Other inputs and management options are summarised in Supplementary Table 6.

In addition to a *baseline* scenario using year 2015 N fertiliser application rates, we ran simulations for a range of other N fertiliser input rates. These additional simulations varied the mineral fertiliser rate between 0 and 600 kgNha⁻¹ cropping-season⁻¹ (specifically we simulated 0, 20, 40, 60, 80, 100, 120, 140, 160, 180, 200, 220, 240, 260, 280, 300, 350, 400, 500, 600 kgNha⁻¹ cropping-season⁻¹).

Rather than just using climate data for 2015, we averaged model outputs over 10 years of climate input (2006–2015). This

was motivated by our aim to capture 2015-like conditions, rather than specifically modelling the year 2015. As such, we aimed to avoid anomalies arising from using only a single year of climate data, for example due to the chance occurrence of (possibly atypical) heavy rainfall shortly after fertilisation, resulting in very high NO₃⁻ leaching.

Model outputs: These included cereal yields, direct N₂O emissions, NO₃⁻ leaching, NH₃ volatilisation, water percolating out of the soil layer and surface runoff. Indirect N₂O emissions were calculated from NO₃⁻ leaching and NH₃ volatilisation using the emission factors given in the 2019 refinement to the 2006 IPCC guidelines⁷⁴ (which estimate that 1.1% of leached NO₃⁻ and 1% of volatilised NH₃ are converted to N₂O). In order to determine the N load of water leaving the field we divided NO₃⁻ leaching by the total volume of water leaving the field (i.e. percolation and surface run-off).

The model outputs were used to create a multidimensional dataset, linking N fertiliser usage to cereal production and N losses. Using this dataset, fertiliser response curves were constructed for every combination of grid cell, crop-type, water management option (rainfed/irrigated) and quantity of interest (cereal yields, N₂O emissions etc.) by interpolating between the 21 simulated N fertiliser levels.

In order to convert per hectare model outputs into total cereal production, N₂O emissions etc., we used grid-cell specific harvested areas. These were based on the MIRCA2000 dataset, which gives rain-fed and irrigated areas for approximately the year 2000⁷⁸. Since worldwide harvested areas have changed considerably in recent years, the harvested areas in the MIRCA2000 dataset were scaled on a country-by-country basis using the FAOSTAT statistics¹⁴. That is, the distribution of cropland within a country, and the irrigated fraction within each grid cell were set to the values in the MIRCA2000 dataset, while the total harvested area for each country was set to the FAO-provided value for 2015. Only grid cells with >500 ha of harvested area were simulated, both to reduce the computational effort and to avoid skewing map-based visualisations of the results towards regions with very little cereal agriculture. As a result, the total simulated area was 566.4 Mha, corresponding to 99% of the total global harvested area for maize, wheat and rice of 574.9 Mha¹⁴.

Targets for 2030: Targets were used to constrain the scenarios discussed in the main text (see Table 1). The predicted increase in crop demand for the period 2015–2030 was adapted from the prediction of a 35–56% increase between 2010 and 2050¹⁸. Taking into account the known increase in crop production between 2010 and 2015¹⁴, and assuming a linear increase in the period 2015–2050, results in an increase of 7–15% for 2015–2030.

N₂O emission targets were adapted from the IPCC report on limiting global warming to 1.5°C²⁴. This includes multiple scenarios for emission reductions, each of which has an associated trajectory for agricultural N₂O emissions in the period 2010–2030. The most extreme of these scenarios (for agricultural N₂O emissions) involves a 26% reduction. A second no-overshoot scenario allows for a 5% increase in N₂O emissions, which is compensated by higher cuts in other greenhouse gas emissions. Taking into account the increase in N fertiliser usage between 2010 and 2015¹⁴, these scenarios are consistent with a 29% decrease or 1% increase in N₂O emissions in the period 2015–2030.

NO₃⁻ leaching targets were adapted from the finding that a N content of 0.5–2.5 mgNl⁻¹ is sufficient to degrade aquatic ecosystems^{7,9,23}. We adopt the upper end of this range as the maximum allowable leaching rate from cereal agroecosystems and apply it at the grid cell level. We choose the upper end, since water flowing into surface and ground water stores from cereal

agroecosystems will be mixed with that flowing from other land use types, often with lower N concentrations. An important caveat is that equivalent action needs to be taken to limit N losses from livestock production. Our assumption of a globally homogeneous critical load for NO_3^- losses is consistent with past studies^{7,9,43,44}, but, in reality, there will be some heterogeneity (e.g. the presence of wetlands may enhance the ability of a landscape to retain and immobilise excess NO_3^- , thus allowing for a higher critical load⁷⁹). If the NO_3^- leaching target is exceeded despite reducing synthetic N fertiliser application to zero (i.e. due to a combination of soil N mineralisation and manure application) we do not try to enforce the target by other means (e.g. reduced manure application).

Optimising N fertiliser usage: A stochastic minimisation procedure was used to spatially redistribute N fertiliser to minimise its usage for a fixed value of global maize, wheat or rice production. The minimisation was performed subject to the additional condition that NO_3^- leaching losses should not exceed 2.5 mgNl^{-1} in any grid cell (unless they already do so in the absence of synthetic fertiliser application). The process was then repeated for different values of global production. Details of the implementation are given in Supplementary Note 3.

When evaluating global production increases, we aimed to keep the ratio between maize, wheat and rice production fixed at the current level, under the assumption that relative demand for maize, wheat and rice is likely not to change dramatically over the timeframe of our study. However, this was only possible up to a total increase of 9%, at which point no further increase in maize yields was possible (due to a combination of yield saturation and NO_3^- leaching constraints). In consequence, production increases >9% are achieved by increasing rice and wheat yields more than maize yields.

Data availability

Input data is publicly available and listed in Supplementary Table 6. Inputs include soil properties (<https://www.fao.org/soils-portal/data-hub/soil-maps-and-databases/harmonized-world-soil-database-v12/en/>), climate data (https://data.isimip.org/search/page/2/simulation_round/ISIMIP3a/product/InputData/climate_forcing/gswp3-w5e5/query/gswp3-w5e5_obsclim/), N deposition rates (<https://data.isimip.org/search/product/InputData/subcategory/n-deposition/>), N fertiliser application rates (<https://zenodo.org/record/5176008>) and crop calendars (<https://zenodo.org/record/5062513>). The LDNDC results used to create the figures and referenced throughout the text are available via Zenodo⁸⁰ (<https://zenodo.org/record/8214104>).

Code availability

LandscapeDNDC (model website: <https://ldndc.imk-ifu.kit.edu>) is available via the Radar4kit depository⁸¹ (<https://radar.kit.edu/radar/en/dataset/gzeZcaTYNiPMzEyV.LandscapeDNDC%2B%2528v1.30.4%2529>). Codes used for analysis and plotting of all the figures are available via Zenodo (<https://zenodo.org/record/8214104>)⁸⁰.

Received: 19 January 2023; Accepted: 21 August 2023;

Published online: 28 September 2023

References

1. Erisman, J. W., Sutton, M. A., Galloway, J., Klimont, Z. & Winiwarter, W. How a century of ammonia synthesis changed the world. *Nat. Geosci.* **1**, 636–639 (2008).
2. Galloway, J. N. et al. The nitrogen cascade. *BioScience* **53**, 341–356 (2021).
3. Battye, W., Aneja, V. & Schlesinger, W. Is nitrogen the next carbon? *Earths Future* **5**, 894–904 (2017).
4. Scheer, C., Fuchs, K., Pelster, D. E. & Butterbach-Bahl, K. Estimating global terrestrial denitrification from measured $\text{N}_2\text{O}:(\text{N}_2\text{O} + \text{N}_2)$ product ratios. *Curr. Opin. Environ. Sustain.* **47**, 72–80 (2020).
5. Fowler, D. et al. Effects of global change during the 21st century on the nitrogen cycle. *Atmos. Chem. Phys.* **15**, 13849–13893 (2015).
6. Rockström, J. et al. Planetary boundaries: exploring the safe operating space for humanity [Internet]. *Ecol. Soc.* **14**, 32 (2009).
7. de Vries, W., Kros, J., Kroeze, C. & Seitzinger, S. P. Assessing planetary and regional nitrogen boundaries related to food security and adverse environmental impacts. *Curr. Opin. Environ. Sustain.* **5**, 392–402 (2013).
8. Steffen, W. et al. Planetary boundaries: guiding human development on a changing planet. *Science* **347**, 1259855 (2015).
9. Schulte-Uebbing, L. F., Beusen, A. H. W., Bouwman, A. F. & de Vries, W. From planetary to regional boundaries for agricultural nitrogen pollution. *Nature* **610**, 507–512 (2022).
10. Arias, P. A. et al. in *Climate Change 2021: The Physical Science Basis. Contribution of Working Group I to the Sixth Assessment Report of the Intergovernmental Panel on Climate Change.* <https://doi.org/10.1017/9781009157896.002> (2021).
11. Smith, V. H., Tilman, G. D. & Nekola, J. C. Eutrophication: impacts of excess nutrient inputs on freshwater, marine, and terrestrial ecosystems. *Environ. Pollut.* **100**, 179–196 (1999).
12. Rabalais, N. N., Turner, R. E. & Wiseman, W. J. Gulf of Mexico hypoxia, A.K.A. “the dead zone”. *Annu. Rev. Ecol. Syst.* **33**, 235–263 (2002).
13. Carstensen, J., Andersen, J. H., Gustafsson, B. G. & Conley, D. J. Deoxygenation of the Baltic Sea during the last century. *Proc. Natl. Acad. Sci. USA* **111**, 5628–5633 (2014).
14. FAO. FAOSTAT. Rome: Food and Agriculture Organization of the United Nations. (2023).
15. Tilman, D., Balzer, C., Hill, J. & Befort, B. L. Global food demand and the sustainable intensification of agriculture. *Proc. Natl. Acad. Sci. USA* **108**, 20260–20264 (2011).
16. Alexandratos, N. & Bruinsma, J. *World Agriculture Towards 2030/2050: the 2012 Revision.* <https://ideas.repec.org/p/ags/faoes/288998.html> (2012).
17. Hunter, M. C., Smith, R. G., Schipanski, M. E., Atwood, L. W. & Mortensen, D. A. Agriculture in 2050: Recalibrating targets for sustainable intensification. *BioScience* **67**, 386–391 (2017).
18. van Dijk, M., Morley, T., Rau, M. L. & Saghai, Y. A meta-analysis of projected global food demand and population at risk of hunger for the period 2010–2050. *Nat. Food* **2**, 494–501 (2021).
19. FAO. *Global Food Losses and Food Waste—Extent, Causes and Prevention* (OCHA, 2011).
20. Kumm, M. et al. Lost food, wasted resources: global food supply chain losses and their impacts on freshwater, cropland, and fertiliser use. *Sci. Total Environ.* **438**, 477–489 (2012).
21. Willett, W. et al. Food in the Anthropocene: the Lancet Commission on healthy diets from sustainable food systems. *The Lancet* **393**, 447–492 (2019).
22. Haas, E. et al. LandscapeDNDC: a process model for simulation of biosphere–atmosphere–hydrosphere exchange processes at site and regional scale. *Landsc. Ecol.* **28**, 615–636 (2013).
23. Camargo, J. A. & Alonso, Á. Ecological and toxicological effects of inorganic nitrogen pollution in aquatic ecosystems: a global assessment. *Environ. Int.* **32**, 831–849 (2006).
24. Masson-Delmotte, V. et al. *Global Warming of 1.5 °C. An IPCC Special Report on the Impacts of Global Warming of 1.5 °C Above Pre-industrial Levels and Related Global Greenhouse Gas Emission Pathways, in the Context of Strengthening the Global Response to the Threat of Climate Change, Sustainable Development, and Efforts to Eradicate Poverty* (World Meteorological Organization, 2018).
25. Jägermeyr, J. et al. Climate impacts on global agriculture emerge earlier in new generation of climate and crop models. *Nat. Food* **2**, 873–885 (2021).
26. Heinke, J., Müller, C., Mueller, N. D. & Jägermeyr, J. N application rates from mineral fertiliser and manure. *Zenodo* <https://doi.org/10.5281/zenodo.4954582> (2021).
27. Zhang, B. et al. Global manure nitrogen production and application in cropland during 1860–2014: a 5 arcmin gridded global dataset for Earth system modeling. *Earth Syst. Sci. Data* **9**, 667–678 (2017).
28. Tian, H. et al. A comprehensive quantification of global nitrous oxide sources and sinks. *Nature* **586**, 248–256 (2020).
29. WHO. *Guidelines for Drinking-Water Quality: Fourth Edition Incorporating First Addendum*. 541 (WHO, 2017).
30. Mueller, N. D. et al. A tradeoff frontier for global nitrogen use and cereal production. *Environ. Res. Lett.* **9**, 054002 (2014).
31. Mueller, N. D. et al. Declining spatial efficiency of global cropland nitrogen allocation. *Glob. Biogeochem. Cycles* **31**, 245–257 (2017).
32. Puma, M. J., Bose, S., Chon, S. Y. & Cook, B. I. Assessing the evolving fragility of the global food system. *Environ. Res. Lett.* **10**, 024007 (2015).
33. Gaupp, F., Hall, J., Mitchell, D. & Dadson, S. Increasing risks of multiple breadbasket failure under 1.5 and 2 °C global warming. *Agric. Syst.* **175**, 34–45 (2019).

34. Clapp, J. Food self-sufficiency: making sense of it, and when it makes sense. *Food Policy* **66**, 88–96 (2017).
35. Cassman, K. G. Ecological intensification of cereal production systems: yield potential, soil quality, and precision agriculture. *Proc. Natl. Acad. Sci. USA* **96**, 5952–5959 (1999).
36. Cassman, K. G., Dobermann, A., Walters, D. T. & Yang, H. Meeting cereal demand while protecting natural resources and improving environmental quality. *Annu. Rev. Environ. Resour.* **28**, 315–358 (2003).
37. van Ittersum, M. K. et al. Yield gap analysis with local to global relevance—a review. *Field Crops Res.* **143**, 4–17 (2013).
38. Cassman, K. G., Dobermann, A. & Walters, D. T. Agroecosystems, nitrogen-use efficiency, and nitrogen management. *AMBIO J. Hum. Environ.* **31**, 132–140 (2002).
39. Mueller, N. D. et al. Closing yield gaps through nutrient and water management. *Nature* **490**, 254–257 (2012).
40. Liu, W. et al. Achieving high crop yields with low nitrogen emissions in global agricultural input intensification. *Environ. Sci. Technol.* **52**, 13782–13791 (2018).
41. Leitner, S. et al. Closing maize yield gaps in sub-Saharan Africa will boost soil N₂O emissions. *Curr. Opin. Environ. Sustain.* **47**, 95–105 (2020).
42. Smerald, A., Fuchs, K., Kraus, D., Butterbach-Bahl, K. & Scheer, C. Significant global yield-gap closing is possible without increasing the intensity of environmentally harmful nitrogen losses. *Front. Sustain. Food Syst.* <https://doi.org/10.3389/fsufs.2022.736394> (2022).
43. Gerten, D. et al. Feeding ten billion people is possible within four terrestrial planetary boundaries. *Nat. Sustain.* **3**, 200–208 (2020).
44. Chang, J. et al. Reconciling regional nitrogen boundaries with global food security. *Nat. Food* **2**, 700–711 (2021).
45. Johnston, A. M. & Bruulsema, T. W. 4R nutrient stewardship for improved nutrient use efficiency. *Procedia Eng* **83**, 365–370 (2014).
46. Zhang, X. et al. Managing nitrogen for sustainable development. *Nature* **528**, 51–59 (2015).
47. Lugato, E., Leip, A. & Jones, A. Mitigation potential of soil carbon management overestimated by neglecting N₂O emissions. *Nat. Clim. Change* **8**, 219–223 (2018).
48. Haas, E., Carozzi, M., Massad, R. S., Butterbach-Bahl, K. & Scheer, C. Long term impact of residue management on soil organic carbon stocks and nitrous oxide emissions from European croplands. *Sci. Total Environ.* **836**, 154932 (2022).
49. Qiao, C. et al. How inhibiting nitrification affects nitrogen cycle and reduces environmental impacts of anthropogenic nitrogen input. *Glob. Change Biol.* **21**, 1249–1257 (2015).
50. Thapa, R., Chatterjee, A., Awale, R., McGranahan, D. A. & Daigh, A. Effect of enhanced efficiency fertilizers on nitrous oxide emissions and crop yields: a meta-analysis. *Soil Sci. Soc. Am. J.* **80**, 1121–1134 (2016).
51. Oenema, O. & Tamminga, S. Nitrogen in global animal production and management options for improving nitrogen use efficiency. *Sci. China C Life Sci* **48**, 871–887 (2005).
52. Neumann, K., Verburg, P. H., Stehfest, E. & Müller, C. The yield gap of global grain production: a spatial analysis. *Agric. Syst.* **103**, 316–326 (2010).
53. Holligan, A. *Why Dutch Farmers are Protesting Over Emissions Cuts* (BBC News, 2022).
54. Kraus, D. et al. A new LandscapeDNDC biogeochemical module to predict CH₄ and N₂O emissions from lowland rice and upland cropping systems. *Plant Soil* **386**, 125–149 (2015).
55. Molina-Herrera, S. et al. Importance of soil NO emissions for the total atmospheric NO_x budget of Saxony, Germany. *Atmos. Environ.* **152**, 61–76 (2017).
56. Petersen, K. et al. Dynamic simulation of management events for assessing impacts of climate change on pre-alpine grassland productivity. *Eur. J. Agron.* **128**, 126306 (2021).
57. Farquhar, G. D., von Caemmerer, S. & Berry, J. A. A biochemical model of photosynthetic CO₂ assimilation in leaves of C₃ species. *Planta* **149**, 78–90 (1980).
58. Ball, J. T., Woodrow, I. E. & Berry, J. A. in *Progress in Photosynthesis Research: Volume 4 Proceedings of the VIIth International Congress on Photosynthesis Providence, Rhode Island, USA, August 10–15, 1986* (ed. Biggins, J.) 221–224 (Springer Netherlands, 1987).
59. Kiese, R. et al. Quantification of nitrate leaching from German forest ecosystems by use of a process oriented biogeochemical model. *Environ. Pollut.* **159**, 3204–3214 (2011).
60. Kim, Y. et al. Estimation and mitigation of N₂O emission and nitrate leaching from intensive crop cultivation in the Haeen catchment, South Korea. *Sci. Total Environ.* **529**, 40–53 (2015).
61. Molina-Herrera, S. et al. A modeling study on mitigation of N₂O emissions and NO₃ leaching at different agricultural sites across Europe using LandscapeDNDC. *Sci. Total Environ.* **553**, 128–140 (2016).
62. Kraus, D. et al. How well can we assess impacts of agricultural land management changes on the total greenhouse gas balance (CO₂, CH₄ and N₂O) of tropical rice-cropping systems with a biogeochemical model? *Agric. Ecosyst. Environ.* **224**, 104–115 (2016).
63. Kasper, M. et al. N₂O emissions and NO₃ leaching from two contrasting regions in Austria and influence of soil, crops and climate: a modelling approach. *Nutr. Cycl. Agroecosystems* **113**, 95–111 (2019).
64. Kraus, D. et al. Greenhouse gas mitigation potential of alternate wetting and drying for rice production at national Scale—a modeling case study for the Philippines. *J. Geophys. Res. Biogeosci.* **127**, e2022JG006848 (2022).
65. Denk, T. R. A., Kraus, D., Kiese, R., Butterbach-Bahl, K. & Wolf, B. Constraining N cycling in the ecosystem model LandscapeDNDC with the stable isotope model SIMONE. *Ecology* **100**, e02675 (2019).
66. Dirnböck, T., Kobler, J., Kraus, D., Grote, R. & Kiese, R. Impacts of management and climate change on nitrate leaching in a forested karst area. *J. Environ. Manage.* **165**, 243–252 (2016).
67. Cade, S. M. et al. Evaluation of LandscapeDNDC model predictions of CO₂ and N₂O fluxes from an oak forest in SE England. *Forests* <https://doi.org/10.3390/fl2111517> (2021).
68. Rahimi, J. et al. Modelling gas exchange and biomass production in west African Sahelian and Sudanian ecological zones. *Geosci. Model Dev. Discuss* **2021**, 1–39 (2021).
69. Houska, T. et al. Rejecting hydro-biogeochemical model structures by multi-criteria evaluation. *Environ. Model. Softw.* **93**, 1–12 (2017).
70. Houska, T., Kraus, D., Kiese, R. & Breuer, L. Constraining a complex biogeochemical model for CO₂ and N₂O emission simulations from various land uses by model–data fusion. *Biogeosciences Online* **14**, 3487–3508 (2017).
71. Ibraim, E. et al. Denitrification is the main nitrous oxide source process in grassland soils according to quasi-continuous isotopocule analysis and biogeochemical modeling. *Glob. Biogeochem. Cycles* **34**, e2019GB006505 (2020).
72. Klatt, S. et al. in *Synthesis and Modeling of Greenhouse Gas Emissions and Carbon Storage in Agricultural and Forest Systems to Guide Mitigation and Adaptation* 149–171 (John Wiley & Sons, Ltd, 2016).
73. Butterbach-Bahl, K. et al. Activity data on crop management define uncertainty of CH₄ and N₂O emission estimates from rice: a case study of Vietnam. *J. Plant Nutr. Soil Sci.* **185**, 793–806 (2022).
74. IPCC. *2019 Refinement to the 2006 IPCC Guidelines for National Greenhouse Gas Inventories* (IPCC, 2019).
75. GAEZ. IASA/FAO, 2012. *Global Agroecological Zones (GAEZ v3.0)* (IIASA, 2012).
76. Morais, T. G., Teixeira, R. F. M. & Domingos, T. Detailed global modelling of soil organic carbon in cropland, grassland and forest soils. *PLoS One* **14**, 1–27 (2019).
77. Hurtt, G. C. et al. Harmonization of global land use change and management for the period 850–2100 (LUH2) for CMIP6. *Geosci. Model Dev.* **13**, 5425–5464 (2020).
78. Portmann, F. T., Siebert, S. & Döll, P. MIRCA2000—Global monthly irrigated and rainfed crop areas around the year 2000: a new high-resolution data set for agricultural and hydrological modeling. *Glob. Biogeochem. Cycles* <https://doi.org/10.1029/2008GB003435> (2010).
79. Houlton, B. et al. A world of cobenefits: solving the global nitrogen challenge. *Earths Future* **7**, 865–872 (2019).
80. Smerald, A. Data and plotting scripts: achieving food security within environmental boundaries through global redistribution of nitrogen fertiliser. *Zenodo* <https://doi.org/10.5281/zenodo.8214104> (2023).
81. Butterbach-Bahl, K. et al. *LandscapeDNDC (v1.30.4)*. <https://doi.org/10.35097/438> (2021).

Acknowledgements

The authors acknowledge funding by the German Federal Ministry of Education and Research (BMBF) under the Make our Planet Great Again—German Research Initiative, Grant Number 306060, implemented by the German Academic Exchange Service (DAAD). The authors also acknowledge support by the state of Baden-Württemberg through bwHPC.

Author contributions

A.S. designed the study with input from C.S., J.R., K.B.-B., K.F. and R.K. The simulations were carried out by A.S., with support from D.K. A.S. conducted the data analysis and wrote the manuscript, with help from all the authors.

Funding

Open Access funding enabled and organized by Projekt DEAL.

Competing interests

The authors declare no competing interests.

Additional information

Supplementary information The online version contains supplementary material available at <https://doi.org/10.1038/s43247-023-00970-8>.

Correspondence and requests for materials should be addressed to Andrew Smerald.

Peer review information *Communications Earth & Environment* thanks Naiqing Pan, Nimai Senapati and Nathan Mueller for their contribution to the peer review of this work. Primary Handling Editors: Fiona Tang and Aliénor Lavergne. A peer review file is available

Reprints and permission information is available at <http://www.nature.com/reprints>

Publisher's note Springer Nature remains neutral with regard to jurisdictional claims in published maps and institutional affiliations.



Open Access This article is licensed under a Creative Commons Attribution 4.0 International License, which permits use, sharing, adaptation, distribution and reproduction in any medium or format, as long as you give appropriate credit to the original author(s) and the source, provide a link to the Creative Commons licence, and indicate if changes were made. The images or other third party material in this article are included in the article's Creative Commons licence, unless indicated otherwise in a credit line to the material. If material is not included in the article's Creative Commons licence and your intended use is not permitted by statutory regulation or exceeds the permitted use, you will need to obtain permission directly from the copyright holder. To view a copy of this licence, visit <http://creativecommons.org/licenses/by/4.0/>.

© The Author(s) 2023